THE JOURNAL OF BIOLOGICAL CHEMISTRY VOL. 282, NO. 17, pp. 12883–12892, April 27, 2007

Functional Characterization of *cis* and *trans* Activity of the Flavivirus NS2B-NS3 Protease*[S]

Received for publication, December 11, 2006, and in revised form, March 1, 2007 Published, JBC Papers in Press, March 2, 2007, DOI 10.1074/jbc.M611318200

Aloke K. Bera[‡], Richard J. Kuhn[‡], and Janet L. Smith[‡§1]

From the [‡]Department of Biological Sciences, Purdue University, West Lafayette, Indiana 47907 and [§]Life Sciences Institute and Department of Biological Chemistry, University of Michigan, Ann Arbor, Michigan 48109

Flaviviruses are serious human pathogens for which treatments are generally lacking. The proteolytic maturation of the 375-kDa viral polyprotein is one target for antiviral development. The flavivirus serine protease consists of the N-terminal domain of the multifunctional nonstructural protein 3 (NS3) and an essential 40-residue cofactor ($NS2B_{40}$) within viral protein NS2B. The NS2B-NS3 protease is responsible for all cytoplasmic cleavage events in viral polyprotein maturation. This study describes the first biochemical characterization of flavivirus protease activity using full-length NS3. Recombinant proteases were created by fusion of West Nile virus (WNV) $NS2B_{40}$ to full-length WNV NS3. The protease catalyzed two autolytic cleavages. The NS2B/NS3 junction was cleaved before protein purification. A second site at $Arg^{459} \downarrow Gly^{460}$ within the C-terminal helicase region of NS3 was cleaved more slowly. Autolytic cleavage reactions also occurred in NS2B-NS3 recombinant proteins from yellow fever virus, dengue virus types 2 and 4, and Japanese encephalitis virus. C*is* and *trans* cleavages were distinguished using a noncleavable WNV protease variant and two types of substrates as follows: an inactive variant of recombinant WNV NS2B-NS3, and cyan and yellow fluorescent proteins fused by a dodecamer peptide encompassing a natural cleavage site. With these materials, the autolytic cleavages were found to be intramolecular only. Autolytic cleavage of the helicase site was insensitive to protein dilution, confirming that autolysis is intramolecular. Formation of an active protease was found to require neither cleavage of NS2B from NS3 nor a free NS3 N terminus. Evidence was also obtained for product inhibition of the protease by the cleaved C terminus of NS2B.

Most flaviviruses, including West Nile virus (WNV),[2] yellow fever virus (YFV), dengue viruses, and Japanese encephalitis virus (JEV), cause severe human diseases. The plus-sense RNA genome of flaviviruses is a single open reading frame encoding a polyprotein precursor of ~3400 amino acids, consisting of three structural proteins (C, prM, and E) and seven nonstructural replication proteins (NS1, NS2A, NS2B, NS3, NS4A, NS4B, and NS5) (Fig. 1*A*) (1–3). Signal sequences direct the polyprotein into the host endoplasmic reticulum (ER) membrane so that NS1 and the exogenous domains of prM and E are in the lumen; C protein, NS3 and NS5 are cytoplasmic; and proteins NS2A, NS2B, NS4A, and NS4B are predominantly *trans*-membrane. Post-translational processing of the polyprotein, which is required for virus replication, is performed by a viral NS3 protease (4, 5) in the cytoplasm and by host proteases in the ER lumen. NS3 protease activity is dependent upon association with an NS2B cofactor ($NS2B_{40}$), a central 40-amino acid hydrophilic domain within the largely hydrophobic NS2B protein (6–8). The viral NS2B-NS3 protease cleaves the viral polyprotein precursor at the NS2A/NS2B, NS2B/NS3, NS3/NS4A, and NS4B/NS5 junctions (Fig. 1*A*), as well as at internal sites within C, NS2A, NS3, and NS4A (9–12). In general, the viral protease has specificity for two basic residues (Lys-Arg, Arg-Arg, Arg-Lys or occasionally Gln-Arg) at the canonical P2 and P1 positions immediately preceding the cleavage site, followed by a small amino acid (Gly, Ser, or Ala) at the P1′ position (Fig. 1*B*).

The activity of NS2B-NS3 protease has been studied *in vitro* using purified, recombinant protease domains of dengue virus type 2 (DV2) and WNV NS3. These studies employed fusions of the NS2B cofactor peptide to truncated forms of NS3 ($NS3_{pro}$) that included only the N-terminal protease domain, one-third of the full-length NS3, and excluded the C-terminal helicase domain (13–16). Among several fusion peptides tested, Gly_4-Ser-Gly_4 was found to be the optimal linker for DV2 NS2B-$NS3_{pro}$ (17, 18), and several groups have used this Gly_4-Ser-Gly_4 linker peptide for a variety of biochemical and mutagenesis studies of protease specificity (19–22).

Crystal structures of DV2 and WNV protease domains have been reported (23, 24). Crystal structures have also been reported for the helicase domains of YFV and DV2 (25, 26). The protease belongs to the chymotrypsin family with a classic Ser-His-Asp catalytic triad. The catalytic triad is arranged identically in structures with (24) and without (23) the $NS2B_{40}$ cofactor. The $NS2B_{40}$ cofactor contributes to the binding site for the P2 residue of the substrate, based on the structure of WNV NS2B-NS3 protease domain in complex with a substrate-based inhibitor (24).

Here we report single polypeptide variants of NS2B-NS3 protease from five flaviviruses. To our knowledge, this is the first study addressing flavivirus protease activity using the $NS2B_{40}$ cofactor

* This work was supported by National Institutes of Health Grant P01 AI-055672 (to R. J. K. and J. L. S.). The costs of publication of this article were defrayed in part by the payment of page charges. This article must therefore be hereby marked "*advertisement*" in accordance with 18 U.S.C. Section 1734 solely to indicate this fact.

[S] The on-line version of this article (available at http://www.jbc.org) contains supplemental Table 1 and Figs. 1 and 2.

[1] To whom correspondence should be addressed: Life Sciences Institute, University of Michigan, 210 Washtenaw Ave., Ann Arbor, MI 48109. E-mail: JanetSmith@umich.edu.

[2] The abbreviations used are: WNV, West Nile virus; YFV, yellow fever virus; JEV, Japanese encephalitis virus; ER, endoplasmic reticulum; YFP, yellow fluorescent protein; CFP, cyan fluorescent protein; DV, dengue virus.

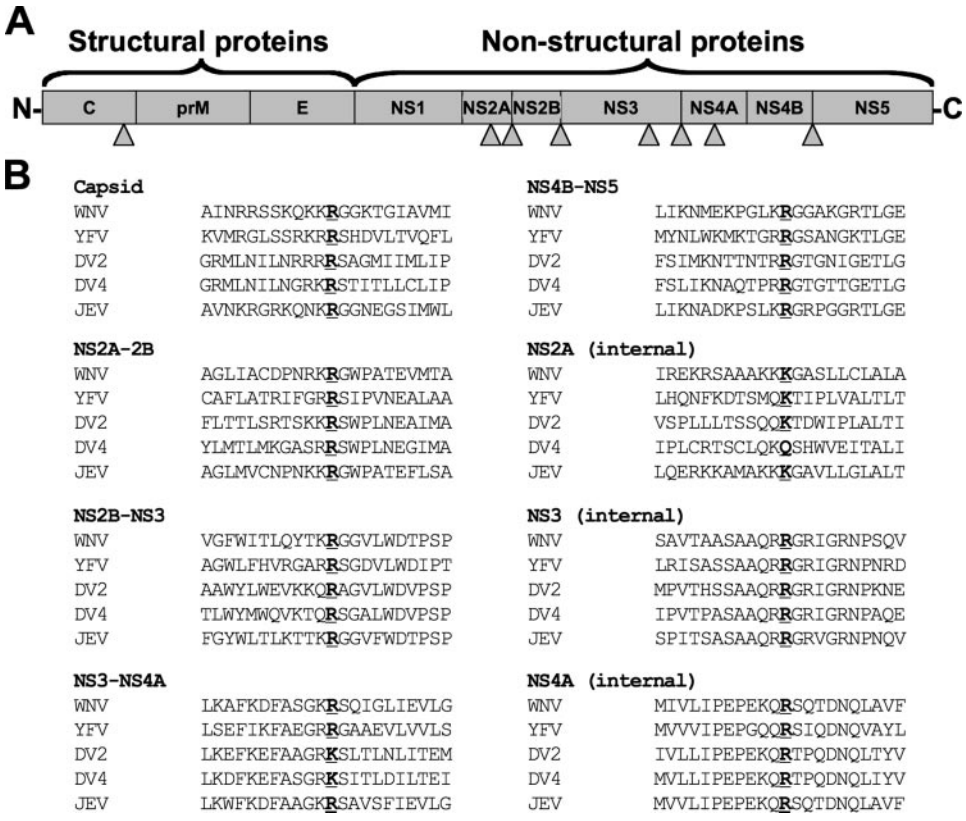

FIGURE 1. **Flavivirus protease cleavage sites.** *A,* schematic diagram of the polyprotein with cleavage sites for the viral protease indicated by *solid arrowheads. B,* sequences of cleavage sites for flavivirus NS2B-NS3 proteases. Cleavage by the viral protease occurs after the *boldface underlined* residue in the "P1" position, in most cases *R.*

and full-length NS3. Detailed experiments on the WNV protease demonstrated that the NS2B/NS3 junction and the internal NS3 site are cleaved in *cis* only. In some variants, product inhibition by the NS2B C terminus was also observed.

MATERIALS AND METHODS

Plasmid Construction—Constructs encoding WNV (strain NY99) proteins were derived from pWN-CG (27), a kind gift of Richard Kinney, Centers for Disease Control and Prevention. For the fusion of the C-terminal 79 residues (residues 53–131) of NS2B with full-length NS3, a 2154-nucleotide fragment was amplified from pWN-CG, using primers WNV-NS2B$_{53}$-F and WNV-NS3FL$_{619STOP}$-R (supplemental Table 1), and cloned between NdeI and BamHI restriction sites in pET28 (Stratagene) to generate pNS2B$_{53-131}$-NS3$_{FL}$ (simply pWNV-NS2B$_{79}$-NS3$_{FL}$). Other WNV plasmids were constructed in two steps. First, an 1857-nucleotide fragment was amplified from pWN-CG by primers WNV-NS3$_1$-F and WNV-NS3$_{619STOP}$-R and cloned into pET28 between NdeI and BamHI restriction sites to generate pWNV-NS3$_{FL}$ encoding full-length NS3. Then fragments encoding the 41-residue protease cofactor within NS2B (residues 53–93) were amplified from pWN-CG using primers WN-NS2B$_{53}$-F and either WNV-NS2B$_{93}$-R or WNV-NS2B$_{95}$-G$_4$SG$_4$-R. The fragments were digested with NdeI and cloned into NdeI-restricted pWNV-NS3$_{FL}$ to generate either pWNV-NS2B$_{53-93}$-HM-NS3$_{FL}$ (simply pWNV-NS2B$_{40}$-HM-NS3$_{FL}$) or pWNV-NS2B$_{53-95}$-G$_4$SG$_4$-HM-NS3$_{FL}$ (simply pWNV-NS2B$_{40}$-G$_4$SG$_4$-HM-NS3$_{FL}$).

Plasmids encoding the active proteases for YFV (pYFV-NS2B$_{40}$-G$_4$SG$_4$-HM-NS3$_{FL}$), DV2 (pDV2-NS2B$_{40}$-G$_4$SG$_4$-ASR-NS3$_{FL}$), dengue virus type 4 (DV4, pDV4-NS2B$_{40}$-G$_4$SG$_4$-HM-NS3$_{FL}$), and JEV (pJEV-NS2B$_{40}$-G$_4$SG$_4$-ASR-NS3$_{FL}$) were constructed in two steps, as described for the WNV protease. PCR primers are listed in supplemental Table 1. For the YFV, and DV4 constructs, an NdeI site between the sequences for the NS2B cofactor and NS3 encoded the amino acids His-Met. For the DV2 and JEV constructs, an NheI site was used, corresponding to Ala-Ser and followed by a basic residue "R," corresponding to the C-terminal residue of NS2B. The plasmid for YFV, pACNR/FLYF (28), was provided by Charles Rice, Laboratory of Virology and Infectious Disease, The Rockefeller University, and plasmids for DV2 and DV4 were from Richard Kinney, and a partial cDNA clone of JEV was from Tsutomu Takegami, Medical Research Institute of Kanazawa Medical University.

Inactive proteases with alanine substitutions at Ser^{135} (WNV, DV2, DV4, and JEV) or Ser^{138} (YFV) in the catalytic triad of NS3 were made by site-directed mutagenesis. For WNV, the substitution was generated by PCR from pWNV-NS2B$_{40}$-G$_4$SG$_4$-HM-NS3$_{FL}$ and primers WNV-S135A-F and WNV-S135A-R, yielding pWNV-NS2B$_{40}$-G$_4$SG$_4$-HM-NS3$_{FL}$/S135A. The PCR product was digested with DpnI before transformation.

The plasmid pCYFP28 encoding cyan (CFP) and yellow fluorescent proteins (YFP) separated by multiple restriction sites was provided by Todd W. Geders (from our laboratory), in the pET28 vector with a C-terminal His tag. The annealed product of S-WNV-2B/3–1 and S-WNV-2B/3–2 (supplemental Table 1) encoding the sequence LQYTKR/GGVLWD between BamHI and HindIII restriction sites was ligated into pCYFP28 to generate pWNV-CFP-LQYTKR/GGVLWD-YFP (or simply pWNV-CFP-2B/3-YFP). Constructs encoding other substrates were made similarly using primers listed in supplemental Table 1. The composition of all constructs was verified by DNA sequencing.

Gene Expression and Protein Purification—The plasmid, pWNV-NS2B$_{40}$-G$_4$SG$_4$-HM-NS3$_{FL}$, was used for high level, inducible expression of N-terminal hexahistidine-tagged recombinant proteins. Cultures of *Escherichia coli* strain Rosetta2 (Novagen) transformed with the expression plasmids were grown in 1 liter of LB medium containing 35 μg/ml chloramphenicol and 50 μg/ml kanamycin at 37 °C until the A_{600} = 0.5. The temperature was reduced to 18 °C, and expression of

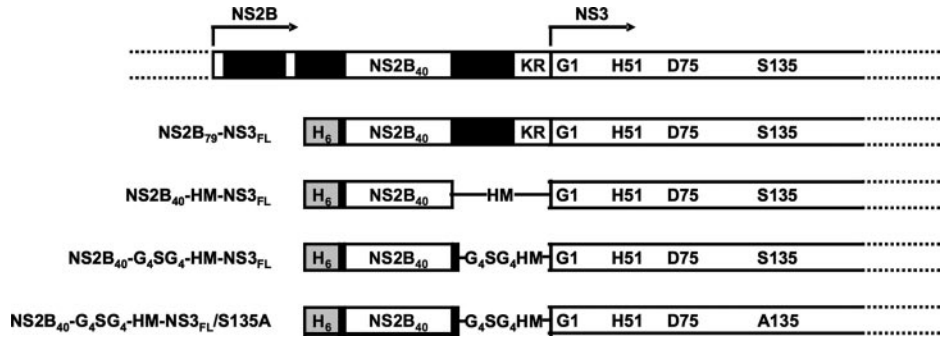

FIGURE 2. **Variants of recombinant West Nile virus NS2B-NS3 used in this study.** *Top row,* NS2B-NS3 region of the viral polyprotein. *Black bars* indicate hydrophobic regions of NS2B that are predicted to be *trans*-membrane. Other rows diagram recombinant proteins. $NS2B_{40}$ represents NS2B residues 54–93, the minimal protease cofactor. $NS3_{FL}$ is the full-length NS3 protein. $NS2B_{40}$ and $NS3_{FL}$ are fused with three different linkers as follows: the natural NS2B C terminus, residues 94–131; *HM*, a 2-residue His-Met linker designed to be uncleavable; and G_4SG_4-*HM*, an 11-residue linker Gly_4-Ser-Gly_4-His-Met. In a final construct, an inactive protease, Ser^{135}–Ala, was created in $NS2B_{40}$-G_4SG_4-HM-$NS3_{FL}$/S135A. *Gray boxes* labeled H_6 represent hexahistidine affinity tags. NS3 residues of the catalytic triad, His^{51} (*H51*), Asp^{75} (*D75*), and Ser^{135} (*S135*) are labeled, as is Gly^{1} (*G1*), the P1′ residue in the N-terminal cleavage site at the NS2B/NS3 junction.

the recombinant protein was induced by addition of isopropyl β-D-thiogalactopyranose to a final concentration of 0.4 mM, cultures were incubated for an additional 12 h at 18 °C, and cells were harvested by centrifugation.

Cell pellets were resuspended in 30 ml of lysis buffer (25 mM sodium phosphate, pH 6.5, 300 mM NaCl, 20 mM imidazole, 5% glycerol), lysed by three passes through a French press at a pressure of 1000 pascals, and centrifuged at 15,000 rpm for 30 min at 4 °C. The supernatant was loaded onto a 5-ml HiTrap chelating column (GE Healthcare) pre-equilibrated with lysis buffer. The column was washed with 30 ml of Buffer A (25 mM Tris-HCl, pH 8.0, 300 mM NaCl, 5% glycerol) containing 50 mM imidazole. The protein was eluted with a linear gradient of 50–300 mM imidazole in Buffer A. Fractions containing NS2B-NS3 proteins, determined by 12% SDS-PAGE, were pooled and dialyzed against Buffer A, first with and then without 2 mM EDTA, concentrated to 10 mg/ml using Centriprep-50 (Millipore), increased to 15% glycerol, and stored at −20 °C. Yields for all WNV protease variants that included 40 residues of the NS2B cofactor were reproducibly 12 mg of purified protein per liter of *E. coli* culture. The variant with 79 residues of NS2B was produced in lower yield. Some proteins (using plasmids pWNV-$NS2B_{79}$-$NS3_{FL}$, pDV2-$NS2B_{40}$-G_4SG_4-ASR-$NS3_{FL}$, and pYFV-$NS2B_{40}$-G_4SG_4-HM-$NS3_{FL}$) were further purified by anion-exchange chromatography. Proteins were dialyzed in 25 mM Tris-HCl, pH 9.0, 75 mM NaCl and 5% glycerol, loaded into a 1-ml HiTrap Q HP column (GE Healthcare), and eluted with a linear gradient of 75–300 mM NaCl.

Protease Assay—For self-cleavage reactions, purified proteins were diluted to the stated concentration (0.25–5.0 mg/ml) in assay buffer (25 mM Hepes, pH 8.5, 50 mM NaCl, 35% glycerol (v/v)), incubated at 37 °C for the indicated times, and quenched by addition of an SDS-PAGE loading buffer to a final concentration of 2% SDS. For intermolecular cleavage reactions, substrate and enzyme were diluted separately to 1 mg/ml in assay buffer, mixed in a 1:4 ratio (enzyme:substrate), unless indicated otherwise, and incubated for the indicated time.

Mass Spectrometry Analysis—The matrix-assisted laser desorption ionization-mass spectrometric results were obtained in the Purdue Campus-wide Mass Spectrometry Facility using an Applied Biosystems (Framingham, MA) Voyager DE PRO mass spectrometer, which uses a nitrogen laser (337 nm) for ionization with a time-of-flight mass analyzer. The positive-ion mass spectra were obtained in the linear mode with an accelerating voltage of 25 kV, a grid voltage of 85%, an extraction delay time of 98 ns, and 150 laser shots per spectrum. The matrix was 2,5-dihydroxybenzoic acid (1 mg/ml in 75% ethanol). Equal volumes of the sample and matrix were mixed and air-dried prior to analysis. The acquisition mass range was 500–10,000 daltons with an instrument error of 0.1%.

RESULTS

Design and Production of Recombinant Flavivirus NS2B-NS3—Flavivirus protease activity is dependent on the association of NS3 with a cofactor ($NS2B_{40}$), a central 40-amino acid hydrophilic domain within the largely hydrophobic NS2B protein. To produce active NS2B-NS3 proteases from five flaviviruses, we engineered proteins in which the 40-residue cofactor from NS2B ($NS2B_{40}$, residues 54–93 of WNV NS2B) was fused to the N terminus of full-length NS3 ($NS3_{FL}$) by a flexible 9-residue linker followed by a noncleavable dipeptide, Gly_4-Ser-Gly_4-His-Met (G_4SG_4-HM) (Fig. 2). A hexahistidine tag was engineered at the N terminus to facilitate purification of NS2B-NS3 protease. Similar recombinant forms of NS2B-NS3 protease were engineered by fusion of the respective NS2B cofactors with NS3 from YFV, DV2, DV4, and JEV. All recombinant proteins were produced in an *E. coli* expression system at 18 °C. The major proportion of the expressed protein was present in the soluble fractions of cell lysate, indicating that recombinant proteins were likely to be folded correctly. The proteins were purified by immobilized metal affinity chromatography via the His_6 tags (in some cases followed by anion-exchange chromatography). SDS-PAGE analysis of purified proteins revealed fragments of lower molecular weight in addition to the expected products (Fig. 3, *lanes 2, 5, 8, 11,* and *14*). These lower molecular weight products increased upon longer incubation at 37 °C (*lanes 3, 6, 9, 12,* and *15*), indicative of proteolysis. However, none of the lower molecular weight fragments was detected in preparations of recombinant proteins in which the protease catalytic serine was substituted with alanine (Fig. 3, *lanes 4, 7, 10, 13,* and *16*) and in which each protein was produced in identical yield to its corresponding parent. Thus, the recombinant NS2B-NS3 protease is subject to autolytic cleavage. At least two sites of autolysis are apparent in most of the NS2B-NS3 proteins,

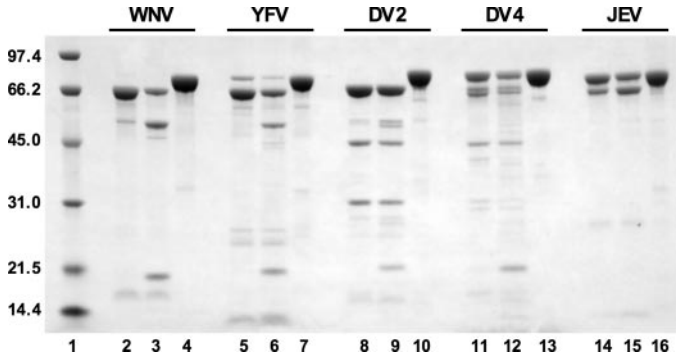

FIGURE 3. **Analysis of five purified recombinant flavivirus NS2B-NS3 proteases.** SDS-PAGE of purified NS2B-NS3 from West Nile virus (*lanes 2–4*), yellow fever virus (*lanes 5–7*), dengue virus type 2 (*lanes 8–10*), dengue virus type 4 (*lanes 11–13*), and Japanese encephalitis virus (*lanes 14–16*). For each recombinant protein, the *1st lane* is freshly purified protein, the *2nd lane* is protein following a 2-h incubation at 37 °C; the *3rd lane* is the purified protease-inactive mutant (S135A or S138A). The active and inactive forms of each protease were produced in equivalent yields. Equivalent amounts of total protein were loaded in all lanes of the gel. The predicted size of the intact recombinant protein is 77 kDa. Molecular mass markers are in *lane 1*. Autolytic cleavage of each of the proteases is apparent.

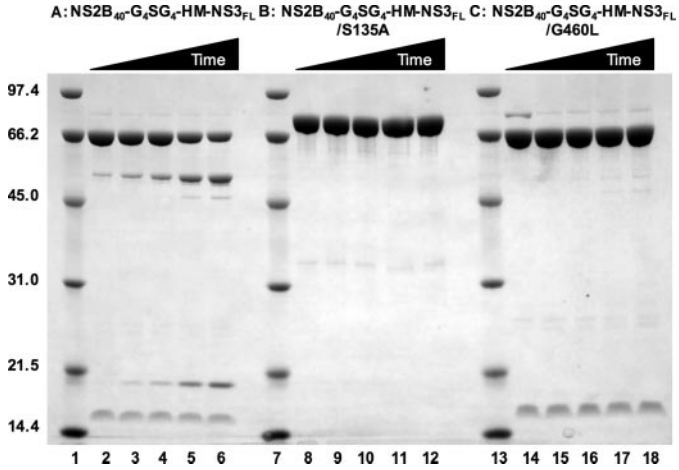

FIGURE 4. **Autolytic cleavage of WNV NS2B-NS3.** Each panel of the SDS-PAGE experiment shows a time course (0, 6, 12, 60, and 120 min) for incubation at 37 °C. The following proteins were examined: the parent enzyme, $NS2B_{40}$-G_4SG_4-HM-$NS3_{FL}$ (*A*); $NS2B_{40}$-G_4SG_4-HM-$NS3_{FL}$/S135A (*B*); and $NS2B_{40}$-G_4SG_4-HM-$NS3_{FL}$/G460L (*C*). Autolytic cleavage (*A*) is confirmed by the S135A substitution at the catalytic residue (*B*). Time-dependent cleavage at $Arg^{459} \downarrow Gly^{460}$ (*A*) is confirmed by the G460L substitution (*C*). The three forms of WNV protease were produced in equivalent yields. Each lane of the gel was loaded with 2.5 μg of protein. Molecular mass markers are in *lanes 1, 7,* and *13*.

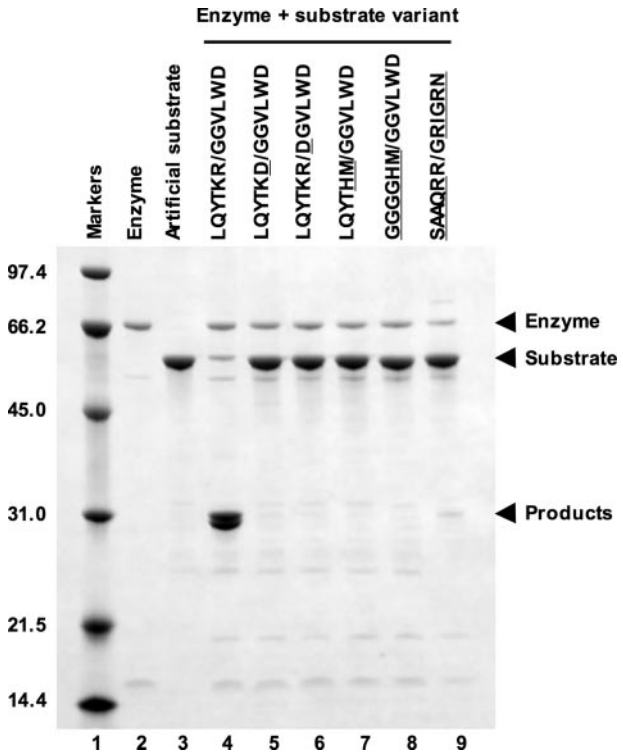

FIGURE 5. **Cleavage of an artificial substrate.** Variants of an artificial substrate were constructed of CFP and YFP fused by a dodecamer peptide. CFP-LQYTKR ↓ GGVLWD-YFP (*lane 3*) contains the wild type NS2B/NS3 junction. The purified parent enzyme, $NS2B_{40}$-G_4SG_4-HM-$NS3_{FL}$ (*lane 2*), was used in cleavage reactions (6 min at 37 °C) with the indicated substrate variants (*lanes 4–9*). The artificial substrate containing the natural NS2B/NS3 junction was cleaved efficiently (*lane 4*), whereas variants with negative charge at the cleavage site (*lanes 5* and *6*) or with sequences from the sites of autolytic cleavage (*lanes 7–9*) were not cleaved in the artificial substrate.

although the five proteases differ in their susceptibility to autolytic cleavage. Further analysis of cleavage was performed using the WNV $NS2B_{40}$-G_4SG_4-HM-$NS3_{FL}$ protein.

Sites of Autolytic Cleavage of WNV NS2B-NS3—Fragments of 8, 18.5, 50.5, and 69 kDa were detected in the recombinant NS2B-NS3 protein from WNV, indicative of two cleavage sites in the full-length protein of 77 kDa (Figs. 3 and 4). These sites were cleaved at different rates. One site was cleaved completely prior to purification, yielding fragments of 69 and 8 kDa (Fig. 4*A*, *lane 2*). Cleavage of the 69-kDa fragment at a second site was slower, as seen at time points during incubation at 37 °C (Fig. 4*A*, *lanes 2–6*). All fragments were associated with the natively folded protein because they did not dissociate upon additional steps of nickel-affinity, anion-exchange, and size-exclusion chromatography of the monomeric protein (supplemental Fig. 1).

To identify the site of rapid cleavage, NS2B-NS3 was analyzed by mass spectrometry. A fragment of 7870 ± 8 Da was identified, which corresponds to cleavage at the "noncleavable" junction following the Gly_4-Ser-Gly_4-His-Met linker between NS2B and NS3 (compared with 7863 Da, calculated mass; data not shown). The cleavage site was also identified by N-terminal sequencing of the 69-kDa fragment, which yielded the sequence Gly-Gly-Val-Leu-Trp-Asp, corresponding to the N terminus of NS3, indicating that cleavage occurs at the site $G_4SG_4HM \downarrow GGVLWD$. Mutagenesis at this site, for experiments described below, provided further confirmation of the site identity. We designate this cleavage as an "N-terminal cleavage." Cleavage at this site was unexpected because the sequence at the site, HM ↓ GG, is unlike the natural cleavage sequences at the critical P1 residue (Met *versus* Arg, see Fig. 1*B*), and substitution of Leu for Arg in the P1 position of the YFV NS2B-NS3 protease domain led to no detectable cleavage (29). In addition, autolytic cleavage of a similar $NS2B_{40}$-fused construct of WNV $NS3_{pro}$ was reported at NS3 residue Lys^{15} (22), in a sequence (KK ↓ G) similar to natural flavivirus protease sites. We anticipated cleavage at Lys^{15}–Gly^{16} when we detected the 8-kDa fragment, and we engineered a protein in which the nonconserved Gly^{16} was substituted with Leu. This substitution had

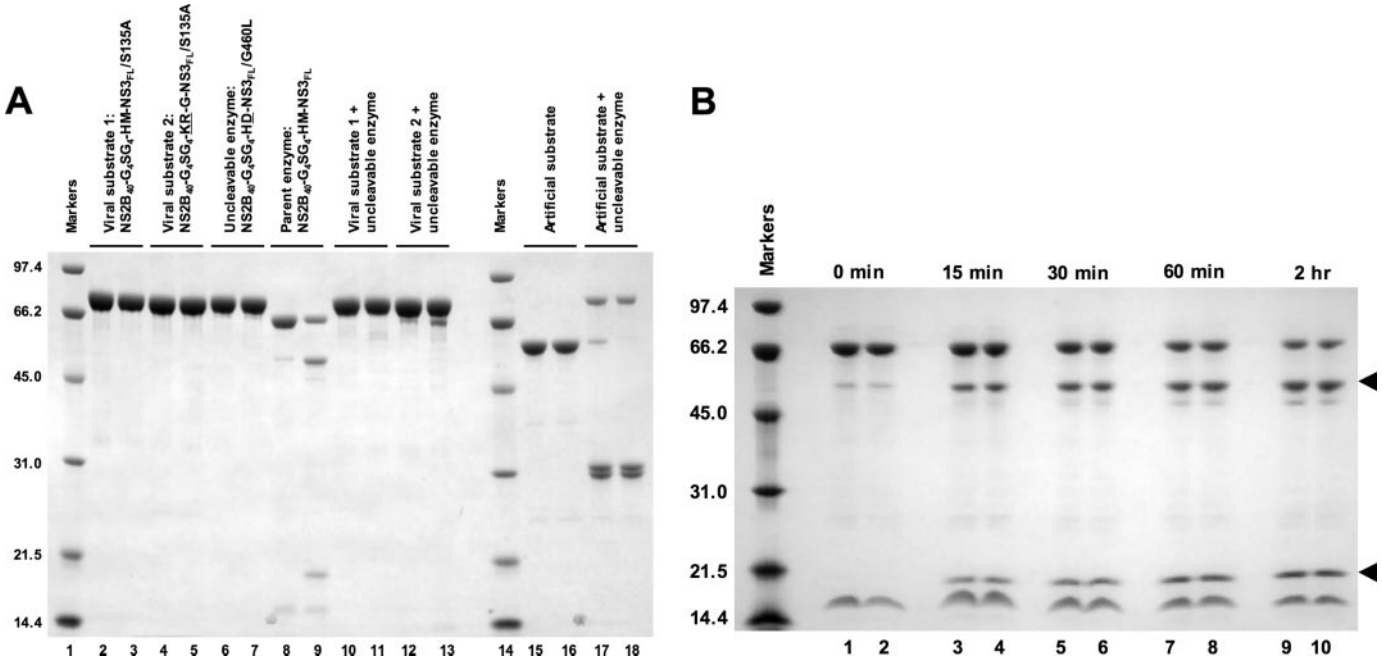

FIGURE 6. **Intramolecular (*cis*) cleavage of NS2B-NS3.** *A,* lack of *trans* cleavage. Two viral substrates lacking catalytic activity (S135A, *lanes 2–5*) and an uncleavable enzyme with substitutions at the sites of autolysis (M-1D/G460L, *lanes 6* and *7*) were not susceptible to autolytic cleavage, whereas the parent enzyme (*lanes 8* and *9*) was cleaved as in Fig. 4. For each protein (1 mg/ml), the *1st lane* (*lanes 2, 4, 6,* and *8*) is as purified, and the *2nd lane* is following a 2-h incubation at 37 °C (*lanes 3, 5, 7,* and *9*). The viral substrates were not cleaved in *trans* by the uncleavable enzyme after 12-min (*lanes 10* and *12*) and 2-h (*lanes 11* and *13*) incubations at 37 °C. The viral substrate with Lys-Arg at the P2-P1 site was cleaved slightly (<5%) at the N-terminal site after the 2 h of incubation (*lane 13*), far below the level of autolytic cleavage (*lanes 8* and *9*). In a positive control for catalytic activity of the uncleavable enzyme, an artificial substrate (CFP-LQYTKR ↓ GGVLWD-YFP *lanes 15* and *16* as purified and after a 2-h incubation at 37 °C) was cleaved efficiently in 12-min (*lane 17*) and 2-h (*lane 18*) incubations at 37 °C. *B, cis* cleavage at the helicase site. The SDS-polyacrylamide gel shows a time course for parallel 37 °C incubations of two $NS2B_{40}$-G_4SG_4-HM-$NS3_{FL}$ samples that differed 20-fold in concentration. For each time point, the *left lane* shows protein from a 0.25 mg/ml incubation (*lanes 1, 3, 5, 7,* and *9*), and the *right lane* shows protein from a 5.0 mg/ml incubation (*lanes 2, 4, 6, 8,* and *10*). Each lane was loaded with 1.7 μg of total protein. Molecular weight markers are at the *left*. *Arrows* indicate the positions of the two fragments produced by cleavage of the helicase site. The N-terminal site is fully cleaved when the protein is purified, yielding the top- and bottom-most bands in each lane.

no impact on appearance of the 8-kDa fragment (data not shown). We conclude that the Lys^{15}–Gly^{16} site is less accessible to the protease active site in full-length NS3 than it is in the isolated protease domain ($NS3_{pro}$). We also attempted to isolate the full-length NS2B-NS3 protein by including protease inhibitors in the lysis buffer for cells from a fresh culture, but the protein was fully cleaved when it emerged from *E. coli* (supplemental Fig. 2).

The second, slower autolytic cleavage was presumed to occur within the helicase domain, where NS3 cleavage has been reported in cells infected with DV2 (10, 12), at a site corresponding to Arg^{459}–Gly^{460} in WNV NS3. Cleavage at this site was confirmed by N-terminal sequencing of the C-terminal fragment. The resulting sequence, Gly-Arg-Ile-Gly-Arg, corresponded to NS3 residues 460–464. The cleavage site was also confirmed by mutagenesis to produce the G460L substitution. The 8- and 69-kDa fragments were present in the purified proteins, but the 18.5- and 50.5-kDa fragments were not detected for $NS2B_{40}$-G_4SG_4-HM-$NS3_{FL}$/G460L (Fig. 4*C*, *lanes 14–18*), confirming that the slower cleavage occurs in the helicase region at Arg^{459} ↓ Gly^{460}. We designate this as the internal helicase site. No autolytic cleavages were observed with enzymatically inactive $NS2B_{40}$-G_4SG_4-HM-$NS3_{FL}$/S135A (Fig. 4*B*, *lane 8–12*).

An Artificial Substrate to Study Cleavage Specificity—To examine the unexpected N-terminal cleavage, we created an artificial substrate containing several variants of the natural NS2B-NS3 cleavage sequence (Fig. 1*B*). In this construct, a dodecapeptide encompassing the natural NS2B/NS3 junction was engineered between two fluorescent proteins, CFP and YFP, to create "CFP-2B/3-YFP" ($LQYTKR^{P1}$ ↓ $G^{P1'}$GVLWD). Proteolytic activity with this substrate was assayed by SDS-PAGE analysis of the reaction mixture, in which substrate (59.3 kDa, Fig. 5, *lane 3*), enzyme (*lane 2*), and two products (29.5 and 29.8 kDa, Fig. 5, *lane 4*) were easily distinguished, or by cleavage-induced loss of fluorescence resonance energy transfer between CFP and YFP (data not shown). We also made several artificial substrates containing substitutions in the NS2B/NS3 junction to check cleavage specificity. The artificial substrate (CFP-LQYTKR ↓ GGVLWD-YFP) containing the natural sequence of the NS2B/NS3 junction was cleaved efficiently (Fig. 5, *lane 4*). Substitution of Asp for Arg at the P1 position (Fig. 5, *lane 5*) or Asp for Gly at the P1′ position (*lane 6*) abolished the cleavage activity. Two artificial substrates containing HM ↓ GG, the site that was cleaved rapidly in the full-length enzyme, were also tested. Neither CFP-LQYTHMGGVLWD-YFP, containing the natural NS2B/NS3 junction with KR replaced by HM, nor CFP-GGGGHMGGVLWD-YFP, containing the junction sequence from our recombinant enzyme, was cleaved in the artificial substrate (Fig. 5, *lanes 7* and *8*). This suggests that either HM ↓ GG is not a substrate for intermolecular cleavage or that a cleavage-competent conformation of HM ↓ GG is not accessible in the context of the artificial

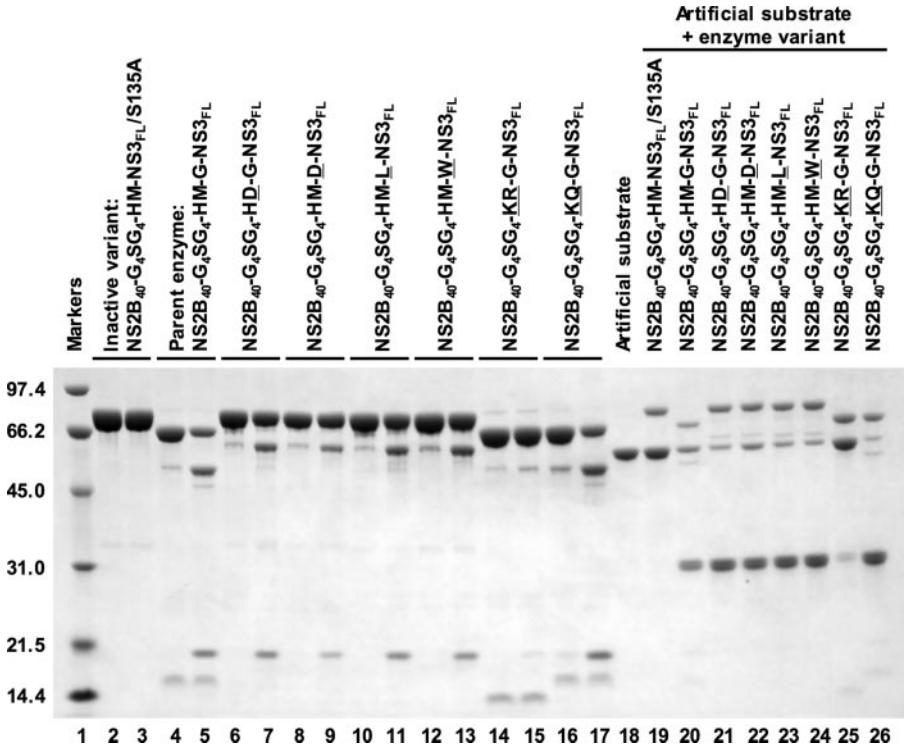

FIGURE 7. **Activity of enzymes with variant NS2B/NS3 junctions.** Variants of the parent enzyme ($NS2B_{40}$-G_4SG_4-HM-$G^{P1'}$-$NS3_{FL}$) were tested for autolytic cleavage activity (*lanes 2–17*). For each of the indicated enzyme variants, each protein is shown first as purified and second after a 2-h incubation at 37 °C. Except for the parent enzyme, all variants with non-natural sequences at the NS2B/NS3 junction were susceptible to autolysis at the helicase site but not at the N-terminal site (*lanes 6–13*). Variants with natural sequences at the NS2B/NS3 junction cleaved both sites (*lanes 14–17*). An artificial substrate (CFP-LQYTKR ↓ GGVLWD-YFP, *lane 18*) was cleaved in *trans* by all variants (*lanes 20–26*) except the negative control (*lane 19*). The variant with the natural sequence at the NS2B/NS3 junction, $NS2B_{40}$-G_4SG_4-KR-G-$NS3_{FL}$, had weak autolytic (presumably *cis*) activity at the helicase site (*lane 15*) and also weak *trans* activity (*lane 25*).

substrate. The natural cleavage sites (Fig. 1*B*) for flavivirus NS2B-NS3 proteases generally have two basic residues (Arg-Arg, Arg-Lys or Lys-Arg) at the P2 and P1 positions and a small amino acid (Gly, Ser, or Ala) at the P1′ position. In contrast to the N-terminal HM ↓ GG cleavage site, the internal helicase cleavage site has a sequence very similar to the natural inter-protein sites (Fig. 1*B*). We also made an artificial substrate, CFP-SAAQRR ↓ GRIGRN-YFP, containing the Arg^{459} ↓ Gly^{460} cleavage site observed in the recombinant protein. However, cleavage of this artificial substrate was barely detectable (Fig. 5, *lane 9*). In the context of the artificial substrate, efficient cleavage of the natural NS2B-NS3 site is in striking contrast to the lack of cleavage of the two sites of autolysis, suggesting that the autolytic reactions may occur in *cis*. Thus we designed materials to test this possibility explicitly.

Intramolecular Proteolytic Cleavage of WNV NS2B-NS3—To determine whether the autolytic cleavage is intramolecular (*cis*) or intermolecular (*trans*), we designed, expressed, and purified a natural substrate for *trans* cleavage (Fig. 6*A*). The protein, $NS2B_{40}$-G_4SG_4-HM-$NS3_{FL}$/S135A, has intact N-terminal and helicase cleavage sites but lacks the protease catalytic side chain (Ser^{135}). $NS2B_{40}$-G_4SG_4-HM-$NS3_{FL}$/S135A undergoes no autolytic cleavage (Fig. 6, *lane 3*) in 2 h at 37 °C, whereas autolysis by the parent enzyme ($NS2B_{40}$-G_4SG_4-HM-$NS3_{FL}$) results in complete cleavage at the N-terminal site and more than 50% cleavage at the internal helicase site under the same conditions (*lane 9*). We also designed, expressed, and purified an enzyme lacking both of the N-terminal and internal cleavage sites ($NS2B_{40}$-G_4SG_4-HD-$NS3_{FL}$/G460L). This protein undergoes no autolytic cleavage (Fig. 6, *lanes 6* and *7*), as expected, but is an efficient enzyme against the artificial substrate CFP-LQYTKR ↓ GGVLWD-YFP (*lanes 17* and *18*). To detect intermolecular hydrolysis, the substrate, $NS2B_{40}$-G_4SG_4-HM-$NS3_{FL}$/S135A, was incubated with the enzyme, $NS2B_{40}$-G_4SG_4-HD-$NS3_{FL}$/G460L. We observed no *trans* cleavage of substrate $NS2B_{40}$-G_4SG_4-HM-$NS3_{FL}$/S135A (Fig. 6, *lanes 10* and *11*) by enzyme $NS2B_{40}$-G_4SG_4-HD-$NS3_{FL}$/G460L under conditions in which this enzyme completely hydrolyzed the artificial substrate (*lanes 17* and *18*). These results clearly indicate intramolecular cleavage of both the N-terminal site (GGGGHM ↓ GGVLWD) and the internal helicase site (SAAQRR ↓ GRIGRN) of recombinant NS2B-NS3. The natural cleavage sequence at the NS2B/NS3 junction was also tested for *trans* cleavage by construction of the substrate $NS2B_{40}$-G_4SG_4-KR-$NS3_{FL}$/S135A. A low level of N-terminal cleavage was seen using the *trans* substrate (Fig. 6, *lanes 12* and *13*), but this was far below the rate of *cis* cleavage of the parent construct (*lanes 8* and *9*). Further confirmation of *cis* cleavage was provided by a dilution experiment using purified $NS2B_{40}$-G_4SG_4-HM-$NS3_{FL}$. The rate of cleavage of the Arg^{459} ↓ Gly^{460} helicase site was independent of a 20-fold difference in protease concentration, as expected for an intramolecular reaction (Fig. 6*B*).

Comparison of Cis and Trans Cleavage Activities in Mutant Proteases—We next examined how a variety of sequences at the NS2B-NS3 cleavage site in a natural substrate affect autolytic cleavage and *trans* cleavage of an artificial substrate (Fig. 7). Several enzymes were made with mutations at the P1 and P1′ positions of the N-terminal cleavage site ($G_4SGGGGHM^{P1}$ ↓ $G^{P1'}$ GVLWD). Substitution of a negatively charged side chain (Asp) at the P1 site or P1′ site, or substitution of a large side chain (Leu or Trp) at the P1′ site, eliminated autolytic cleavage at the NS2B/NS3 junction (Fig. 7, *lanes 6–13*). All enzymes that were not susceptible to N-terminal autolytic cleavage at the NS2B/NS3 junction had efficient *trans* cleavage activity with the artificial *trans* substrate, CFP-LQYTKR ↓ GGVLWD-YFP (*lanes 21–24*), and efficient *cis* cleavage of the internal helicase site (Fig. 7, *lanes 7, 9, 11,* and *13*). This demonstrates that prote-

ase activity requires neither cleavage of NS2B from NS3 nor a free NS3 N terminus. Previous results have been mixed in this regard. Pugachev *et al.* (30) suggested that NS2B-NS3 cleavage is required to release NS3 for internal cleavage at the helicase site. However, Teo and Wright (12) demonstrated that prior cleavage between NS2B and NS3 was not necessary for NS2B-NS3 protease activity.

$NS2B_{40}$-G_4SG_4-KR-$NS3_{FL}$, with the wild type sequence at the NS2B/NS3 junction, had the expected autolytic cleavage at the N-terminal site (Fig. 7, *lane 14*). However, compared with the $NS2B_{40}$-G_4SG_4-HM-$NS3_{FL}$ parent, $NS2B_{40}$-G_4SG_4-KR-$NS3_{FL}$ exhibited unexpectedly low levels of cleavage at the helicase site (Fig. 7, compare *lanes 5* and *15*) and with the *trans* substrate CFP-LQYTKR ↓ GGVLWD-YFP (compare *lanes 20* and *25*). This is in contrast to substitution of Gln for Arg at the cleavage site, which resulted in efficient *cis* (Fig. 7, *lane 17*) and *trans* cleavage (*lane 26*). The simplest explanation of these data is a form of product inhibition, in which the reaction product Lys-Arg-COO^- remains in the P2-P1 site after cleavage and effectively blocks the active site for both *cis* and *trans* substrates.

Effect of Linker Length on Catalytic Activity of NS2B-NS3—We next examined whether Gly_4-Ser-Gly_4, the artificial linker peptide tethering the NS2B cofactor to NS3, was responsible for the unexpectedly low cleavage activity of $NS2B_{40}$-G_4SG_4-KR-$NS3_{FL}$. The effect of the length of the $NS2B_{40}$-NS3 linker on protease activity was studied in proteins having linkers longer and shorter than the Gly_4-Ser-Gly_4 linker of the parent protein, $NS2B_{40}$-G_4SG_4-HM-$NS3_{FL}$ (Fig. 8). We engineered $NS2B_{79}$-$NS3_{FL}$, in which the 38 residues of the natural C terminus of NS2B replaced Gly_4-Ser-Gly_4-HM and were fused to NS3 as in the wild type polyprotein. This region of NS2B is hydrophobic and presumably tethers the C terminus of the 40-residue protease cofactor to the ER membrane. Although $NS2B_{79}$-$NS3_{FL}$ exhibited poor solubility and was difficult to purify (Fig. 8, *lane 4*), it had levels of autolytic (*lane* 5) and *trans* cleavage (*lane 13*) comparable with those of the parent enzyme (*lanes 3* and *12*). We also engineered $NS2B_{40}$-HM-$NS3_{FL}$ and $NS2B_{40}$-KR-$NS3_{FL}$, in which the Gly_4-Ser-Gly_4 linker was absent and the $NS2B_{40}$ cofactor was linked directly to NS3 via HM or KR, respectively. $NS2B_{40}$-HM-$NS3_{FL}$ displayed no autolytic cleavage (Fig. 8, *lanes 8* and *9*) and has barely detectable *trans* cleavage activity (*lane 15*). In contrast, $NS2B_{40}$-KR-$NS3_{FL}$ had both *cis* and *trans* cleavage activities (Fig. 8, *lanes 6, 7,* and *14*) comparable with the parent enzyme (*lanes 2, 3* and *12*). The putative product inhibition by Lys-Arg-COO^- was not observed in $NS2B_{79}$-$NS3_{FL}$ or in $NS2B_{40}$-KR-$NS3_{FL}$.

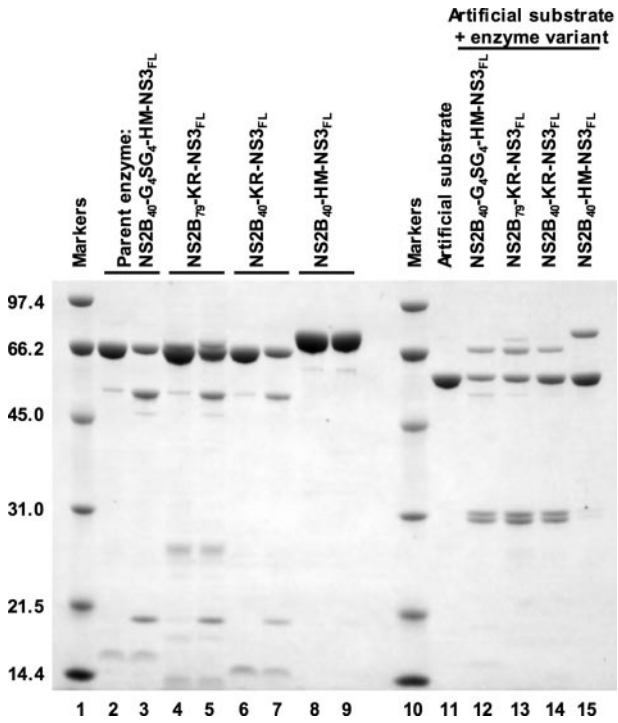

FIGURE 8. **Effect of NS2B-NS3 linker length on protease activity.** Enzyme variants with NS2B-NS3 linkers that were 9 residues shorter (*lanes 6–9*) or 30 residues longer (*lanes 4* and *5*) than the parent (*lanes 2* and *3*) were tested for autolysis (*lanes 2–9*) and for *trans* cleavage (*lanes 12–15*) of an artificial substrate (CFP-LQYTKR ↓ GGVLWD-YFP, *lane 11*). For each of the indicated enzyme variants (*lanes 2–9*), each protein is shown first as purified and second after a 2-h incubation at 37 °C. The longer variant catalyzed *cis* (*lanes 4* and *5*) and *trans* (*lane 13*) cleavages at comparable levels to the parent (*lanes 2, 3,* and *12*). However, shorter variants lacking the Gly_4-Ser-Gly_4 linker had *cis* or *trans* cleavage activity only if the sequence at the NS2B/NS3 junction was wild type (Lys-Arg, *lanes 6, 7,* and *14*) but not with a non-natural junction sequence (His-Met, *lanes 8, 9,* and *15*).

DISCUSSION

This is the first study to examine the activity of the WNV $NS2B_{40}$-NS3 protease in the context of purified, full-length NS3 protein. Previous detailed biochemical studies of flavivirus proteases were of truncations (13–16, 19–22) that included only the protease region of NS3 (WNV NS3 residues ~1–180) but lacked the full helicase region (WNV NS3 residues 180–619). The parent protein for our studies, $NS2B_{40}$-G_4SG_4-HM-$NS3_{FL}$, was a fusion of the 40-residue cofactor of NS2B and full-length NS3. A nonapeptide linker (Gly_4-Ser-Gly_4) was selected based on previously reported active fusions of NS2B and NS3 protease domains from DV2 and WNV (17–22). This linker was connected to the N terminus of NS3 with the dipeptide His-Met, which differs from sequences (Lys-Arg) of the natural substrates of WNV NS2B-NS3 protease. The fusion product, $NS2B_{40}$-G_4SG_4-HM-$NS3_{FL}$, was a stable, monomeric protein, in contrast to full-length NS3 in absence of the NS2B cofactor, which exhibited nonspecific aggregation and poor solubility. This is consistent with the crystal structure of the NS2B-NS3 protease domain, in which the NS2B cofactor buries several hydrophobic surface patches as it wraps around the NS3 protease domain (Fig. 9) (24). The importance of hydrophobic contacts between NS2B and the NS3 protease domain was illustrated in a recent site-directed mutagenesis study of the proteins (21).

$NS2B_{40}$-G_4SG_4-HM-$NS3_{FL}$, the parent enzyme for our studies, was susceptible to autolytic cleavage at two sites (Fig. 4). All cleavage fragments remained associated with the protein, as seen by the identical behavior of cleaved and uncleaved proteins upon ion-exchange and gel filtration chromatography (supplemental Fig. 1). The autolytic cleavage reactions were intramolecular (Fig. 6). Although these autolytic reactions were characterized in detail only for WNV NS2B-NS3 protease, they also occurred to varying extents in the YFV, DV2, DV4, and JEV proteases (Fig. 3), where we assume they are also intramolecu-

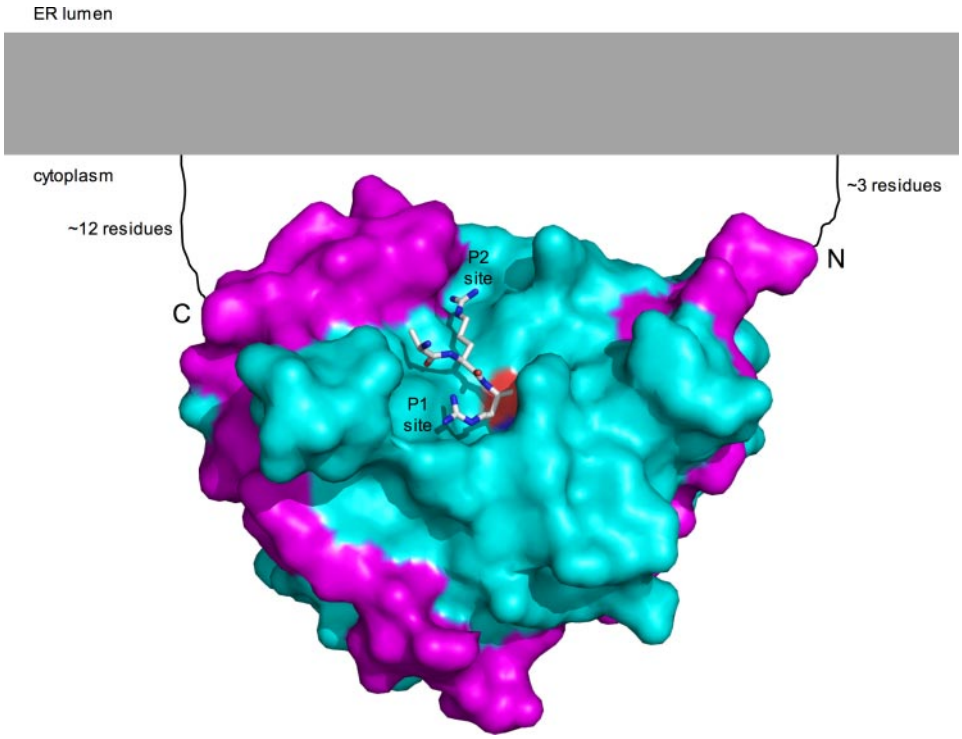

FIGURE 9. **NS2B-NS3 protease domain in relation to the ER membrane (*gray*).** Surfaces of WNV NS3 protease domain (*cyan*) and NS2B cofactor (*magenta*) with bound peptide rendered as *sticks* (Protein Data Bank code 2FP7 (24)). The *red surface* of NS3 is because of the catalytic residue Ser^{135}. Arg side chains in the substrate analog occupy the protease P1 and P2 sites. The NS2B cofactor forms part of the P2 site. The 40-residue cofactor (N and C termini labeled) wraps around the NS3 protease domain like a sling. The NS2B cofactor is preceded and followed by presumed membrane-binding regions of NS2B. The "distances" of the NS2B-NS3 protease to the ER membrane, measured in number of amino acids in NS2B from the *magenta* NS2B cofactor to the nearest hydrophobic region, are marked. The termini of the NS3 protease domain are on the back side of the molecule and not visible in this view.

lar. Indirect evidence, based on the insensitivity of cleavage rates to dilution, has been reported for YFV and DV2 proteases (4, 5), but this is the first direct demonstration of intramolecular (*cis*) cleavage by a flavivirus protease.

Our observation of cleavage at an internal site in the helicase region is consistent with earlier results showing viral protease cleavage at this site in infected cells (10, 12). The new finding here is that the cleavage at $Arg^{459} \downarrow Gly^{460}$ takes place in *cis* only (Fig. 6). The lack of *trans* cleavage of the helicase site (SAAQRR ↓ GRIGRN), in the context of either NS3 (Fig. 6) or an artificial CFP-YFP substrate (Fig. 5), strongly implies *cis* cleavage in infected cells. *Cis* cleavage obviously requires that $Arg^{459} \downarrow Gly^{460}$ be accessible to the protease active site in full-length NS3. If the protease active site is as close to the ER membrane as suggested by Fig. 9, then accessibility may be reduced *in vivo*, accounting for the low levels of NS3 helicase cleavage in infected cells (10, 12). The slower *cis* cleavage of the internal helicase site in comparison to the more rapid cleavage of the NS2B/NS3 junction is also consistent with the crystal structures of YFV and DV2 helicases in which $Arg^{459} \downarrow Gly^{460}$ is part of an α-helix in helicase domain 2 (25, 26). The structure must relax, or unfold slightly, in order for $Arg^{459} \downarrow Gly^{460}$ to be accessible to the protease. $Arg^{459} \downarrow Gly^{460}$ resides within one of the seven highly conserved helicase motifs. The importance, if any, of the internal helicase cleavage to NS3 helicase function or to the virus is unknown.

The internal helicase cleavage site (SAAQRR ↓ GRIGRN) is similar to the other WNV cleavage sites (Fig. 1*B*), and we were surprised that it was not cleaved in *trans*. The main difference to other natural cleavage sites is Arg^{461} at the P2′ position. Lack of *trans* cleavage of this site implies some degree of protease specificity at the P2′ position. Other WNV protease sites have Gly, Gln, or Trp at the P2′ position, although it is unknown whether most of them are cleaved in *cis* or *trans*. Indirect evidence suggests that the NS2A-NS2B site (P2′ Trp) is cleaved in *cis* (5), and the structure of the helicase domain suggests that the NS3-NS4A site is inaccessible for *cis* cleavage and is therefore cleaved in *trans* (25). On this basis, charge rather than size may be the problem with *trans* cleavage of substrates having P2′ Arg.

The cleavage of the noncognate His-Met ↓ Gly at the N-terminal site is attributed to the high effective concentration of a *cis* substrate and to the Gly_4-Ser-Gly_4 linker, which must facilitate binding of His-Met in the protease P2-P1 sites. The situation in the viral polyprotein is more complex. In extensive studies of YFV protease specificity, Rice and co-workers (11, 29, 31) reported high specificity (Arg and Lys) at the P1 position for the NS2A/NS2B and NS2B/NS3 junctions, but more relaxed specificity at the NS3/NS4A (Arg, Lys, Ser, Thr, Ala, Met, and Leu) and NS4B/NS5 (Arg, Lys, Gln, Asn, and His) junctions.

We detected no cleavage at Lys^{15}–Gly^{16} of NS3, as was observed in the variant of the isolated WNV NS2B-NS3 protease domain used for the crystal structure (24). This is easily explained by the structure, in which the first (Thr^{19}) and last (Arg^{170}) ordered residues of the $NS3_{pro}$ domain are less than 20 Å apart. Presumably, the presence of the larger helicase domain (residues 180–619) in full-length NS3 protected Lys^{15}–Gly^{16} from the protease active site.

Our results show that neither cleavage of the NS2B/NS3 junction nor a free NS3 N terminus is required for protease activity. Variants of the parent protein in which *cis* cleavage of NS2B from NS3 was blocked were effective both in *trans* cleavage reactions and in *cis* cleavage of the helicase site (Fig. 7).

Cis cleavage at the N-terminal site of our recombinant proteins depended upon the sequence at the cleavage site and also on the length of the linker between $NS2B_{40}$ and $NS3_{FL}$. The results are easily rationalized by the structure of the WNV NS2B-NS3 protease domain bound to a product analog (24), which shows how the dipeptide Arg-Arg binds in the protease P2-P1 sites (Fig. 9). The distance of peptide

travel would be minimally 20 Å from the last residue of NS2B in the crystal structure (residue 88, labeled *C* in Fig. 9) to the residue in the protease P2 site. In our recombinant proteins, this corresponds to 14 residues in $NS2B_{40}$-G_4SG_4-HM-$NS3_{FL}$ and $NS2B_{40}$-G_4SG_4-KR-$NS3_{FL}$. However, it corresponds to only 5 residues in $NS2B_{40}$-HM-$NS3_{FL}$ and $NS2B_{40}$-KR-$NS3_{FL}$, too few residues to span 20 Å. In recombinant proteins with a 14-residue connector, both noncognate (His-Met) and cognate (Lys-Arg) dipeptides bound productively in the P2-P1 sites, and both $NS2B_{40}$-G_4SG_4-HM-$NS3_{FL}$ and $NS2B_{40}$-G_4SG_4-KR-$NS3_{FL}$ were cleaved in *cis*. However, with the shorter 5-residue connector, only the cognate dipeptide (Lys-Arg) bound productively, so that $NS2B_{40}$-KR-$NS3_{FL}$ was cleaved in *cis* and $NS2B_{40}$-HM-$NS3_{FL}$ was not. This difference is easily explained by residues 83 and 84 near the C terminus of $NS2B_{40}$, which form part of the P2 substrate site (Fig. 9). It may be impossible to form this part of the P2 site and simultaneously place the 10th downstream residue into the P2 site, as would be required with a 5-residue connector. In contrast, the P1 site is formed by NS3 alone (Fig. 9), and binding of *cis* substrates in the P1 site may lead to cleavage even without binding in the P2 site. In $NS2B_{40}$-KR-$NS3_{FL}$, Arg could reach the P1 site, perhaps at the expense of disassembling the P2 site, leading to cleavage. However, in $NS2B_{40}$-HM-$NS3_{FL}$, Met had no intrinsic affinity for the P1 site and was not cleaved. The structure interpretation also explains why $NS2B_{40}$-G_4SG_4-KR-$NS3_{FL}$ was a poor enzyme in our studies. The longer 14-residue connector allowed the cleavage product Lys-Arg-COO^- to remain bound in the P2-P1 sites, effectively blocking other substrates from entering, whereas the shorter 5-residue connector did not allow the product to remain in the active site. Thus, $NS2B_{40}$-KR-$NS3_{FL}$ was a better enzyme than was $NS2B_{40}$-G_4SG_4-KR-$NS3_{FL}$.

The apparent product inhibition by the cognate Lys-Arg dipeptide at the NS2B/NS3 junction of $NS2B_{40}$-G_4SG_4-KR-$NS3_{FL}$ raises the possibility that slow dissociation of the NS2B C terminus from the protease active site may provide a useful pause in viral polyprotein processing. For example, slow dissociation could allow time for downstream events, such as protein folding or protein-protein associations, to occur before further polyprotein processing. Our recombinant NS2B-NS3 proteases differ from the natural situation in two critical ways. First, the NS2B/NS3 junction in our studies was very close to the end of the NS2B cofactor and not separated by the remaining 35 residues of NS2B. No product inhibition was observed in the construct with the full C terminus of NS2B (Fig. 8). Second, in our experiments NS2B was not associated with a biological membrane. Based on predicted membrane domains within NS2B, the distances from the NS2B cofactor to the ER membrane are rather short, ~3 residues from the cofactor N terminus and ~12 residues from the C terminus. If the membrane-associated predictions are correct, then the NS3 protease domain hangs from the ER membrane in a "sling" formed by the NS2B cofactor (Fig. 9). This geometry places the protease active site rather near the ER membrane, no matter how flexible the tethers. This is consistent with positions of the viral protease cleavage sites, which are all proximal to predicted membrane domains of prM, NS2A, NS2B, NS4A, and NS4B.

The results presented here provide new insights into the function of the flavivirus NS3 protease. Differences in the catalytic profile of the protease in full-length NS3 compared with the isolated protease domain are important for protease function in a virus-infected cell.

Acknowledgments—We thank Richard Kinney for kindly providing plasmids encoding the WNV NS2B-NS3, DV2 NS2B-NS3, and DV4 NS2B-NS3; Charles Rice for plasmid encoding the YFV NS2B-NS3; Tsutomu Takegami for providing a partial cDNA clone of JEV; and Todd Geders for providing plasmid pCYFP28.

REFERENCES

1. Brinton, M. A. (2002) *Annu. Rev. Microbiol.* **56,** 371–402
2. Kuhn, R. J., and Strauss, J. H. (2003) *Adv. Protein Chem.* **64,** 363–377
3. Mukhopadhyay, S., Kuhn, R. J., and Rossmann, M. G. (2005) *Nat. Rev. Microbiol.* **3,** 13–22
4. Chambers, T. J., Weir, R. C., Grakoui, A., McCourt, D. W., Bazan, J. F., Fletterick, R. J., and Rice, C. M. (1990) *Proc. Natl. Acad. Sci. U. S. A.* **87,** 8898–8902
5. Preugschat, F., Yao, C. W., and Strauss, J. H. (1990) *J. Virol.* **64,** 4364–4374
6. Chambers, T. J., Grakoui, A., and Rice, C. M. (1991) *J. Virol.* **65,** 6042–6050
7. Falgout, B., Pethel, M., Zhang, Y. M., and Lai, C. J. (1991) *J. Virol.* **65,** 2467–2475
8. Falgout, B., Miller, R. H., and Lai, C. J. (1993) *J. Virol.* **67,** 2034–2042
9. Lin, C., Amberg, S. M., Chambers, T. J., and Rice, C. M. (1993) *J. Virol.* **67,** 2327–2335
10. Arias, C. F., Preugschat, F., and Strauss, J. H. (1993) *Virology* **193,** 888–899
11. Nestorowicz, A., Chambers, T. J., and Rice, C. M. (1994) *Virology* **199,** 114–123
12. Teo, K. F., and Wright, P. J. (1997) *J. Gen. Virol.* **78,** 337–341
13. Yusof, R., Clum, S., Wetzel, M., Murthy, H. M., and Padmanabhan, R. (2000) *J. Biol. Chem.* **275,** 9963–9969
14. Khumthong, R., Angsuthanasombat, C., Panyim, S., and Katzenmeier, G. (2002) *J. Biochem. Mol. Biol.* **35,** 206–212
15. Ganesh, V. K., Muller, N., Judge, K., Luan, C. H., Padmanabhan, R., and Murthy, K. H. (2005) *Bioorg. Med. Chem.* **13,** 257–264
16. Niyomrattanakit, P., Yahorava, S., Mutule, I., Mutulis, F., Petrovska, R., Prusis, P., Katzenmeier, G., and Wikberg, J. E. (2006) *Biochem. J.* **397,** 203–211
17. Leung, D., Schroder, K., White, H., Fang, N. X., Stoermer, M. J., Abbenante, G., Martin, J. L., Young, P. R., and Fairlie, D. P. (2001) *J. Biol. Chem.* **276,** 45762–45771
18. Nall, T. A., Chappell, K. J., Stoermer, M. J., Fang, N. X., Tyndall, J. D., Young, P. R., and Fairlie, D. P. (2004) *J. Biol. Chem.* **279,** 48535–48542
19. Chappell, K. J., Nall, T. A., Stoermer, M. J., Fang, N. X., Tyndall, J. D., Fairlie, D. P., and Young, P. R. (2005) *J. Biol. Chem.* **280,** 2896–2903
20. Li, J., Lim, S. P., Beer, D., Patel, V., Wen, D., Tumanut, C., Tully, D. C., Williams, J. A., Jiricek, J., Priestle, J. P., Harris, J. L., and Vasudevan, S. G. (2005) *J. Biol. Chem.* **280,** 28766–28774
21. Chappell, K. J., Stoermer, M. J., Fairlie, D. P., and Young, P. R. (2006) *J. Biol. Chem.* **281,** 38448–38458
22. Shiryaev, S. A., Ratnikov, B. I., Chekanov, A. V., Sikora, S., Rozanov, D. V., Godzik, A., Wang, J., Smith, J. W., Huang, Z., Lindberg, I., Samuel, M. A., Diamond, M. S., and Strongin, A. Y. (2006) *Biochem. J.* **393,** 503–511
23. Murthy, H. M., Clum, S., and Padmanabhan, R. (1999) *J. Biol. Chem.* **274,** 5573–5580
24. Erbel, P., Schiering, N., D'Arcy, A., Renatus, M., Kroemer, M., Lim, S. P., Yin, Z., Keller, T. H., Vasudevan, S. G., and Hommel, U. (2006) *Nat. Struct. Mol. Biol.* **13,** 372–373
25. Wu, J., Bera, A. K., Kuhn, R. J., and Smith, J. L. (2005) *J. Virol.* **79,** 10268–10277

26. Xu, T., Sampath, A., Chao, A., Wen, D., Nanao, M., Chene, P., Vasudevan, S. G., and Lescar, J. (2005) *J. Virol.* **79,** 10278–10288
27. Beasley, D. W., Whiteman, M. C., Zhang, S., Huang, C. Y., Schneider, B. S., Smith, D. R., Gromowski, G. D., Higgs, S., Kinney, R. M., and Barrett, A. D. (2005) *J. Virol.* **79,** 8339–8347
28. Bredenbeek, P. J., Kooi, E. A., Lindenbach, B., Huijkman, N., Rice, C. M., and Spaan, W. J. (2003) *J. Gen. Virol.* **84,** 1261–1268
29. Chambers, T. J., Nestorowicz, A., and Rice, C. M. (1995) *J. Virol.* **69,** 1600–1605
30. Pugachev, K. V., Nomokonova, N. Y., Dobrikova, E., and Wolf, Y. I. (1993) *FEBS Lett.* **328,** 115–118
31. Lin, C., Chambers, T. J., and Rice, C. M. (1993) *Virology* **192,** 596–604